Entangling an optical cavity and a nanomechanical resonator beam by means of a quantum dot

Xiao-Zhong Yuan*

Department of Physics, Shanghai Jiao Tong University, Shanghai 200240, China

(Received 19 June 2013; revised manuscript received 30 August 2013; published 18 November 2013)

The stationary continuous-variable entanglement between an optical cavity and a nanomechanical resonator beam is generated by their common interaction with a quantum dot. To deal with the quantum dot which is modeled as a two-level system, we do not use the low excitation limit approximation to bosonize the spin operators, but we keep them in the quantum Langevin equations. We linearize the quantum Langevin equations reasonably and investigate the stationary continuous-variable entanglement in detail, and finally we show that a high degree of entanglement can be achieved for experimentally feasible parameters.

DOI: 10.1103/PhysRevA.88.052317 PACS number(s): 03.67.Bg, 42.50.Lc, 85.85.+j

I. INTRODUCTION

Entanglement has been recognized as one of the most amazing aspects of quantum mechanics. It has been considered to be an important resource for applications in quantum communication and information processing, such as quantum teleportation, quantum cryptography, quantum dense coding, and telecloning. Recently, a great deal of attention has been paid to generating entanglement between an optical cavity field and a movable cavity end-mirror [1], between optical and microwave cavity modes [2], between two dielectric membranes suspended inside a cavity [3], between an atomic ensemble inside an optical cavity and a cavity mirror [4], and between two mirrors inside a ring cavity [5]. Also, Ref. [6] considers a two-level atom in a cavity with a thin vibrating end mirror. The bipartite and tripartite continuous variable entanglement among the system is investigated in detail. However, to deal with the two-level atom, the low excitation limit approximation is used to bosonize the spin operators. Reference [7] entangles two optomechanical oscillators as well as two-mode fields via three-level cascade atoms. To deal with the spin operators in some multiplying terms, a zero-order approximation is used. Reference [8] designs an ingenious device to generate multicolor quadripartite entangled beams of light with continuous variables. The entanglement produced can still persist for the environment temperature up to about 50 K. Furthermore, Ref. [9] gives a proposal to generate steady-state optomechanical entanglement at room temperature. It shows us a system consisting of a high-Q_m nanostring oscillator and a high-Q_o microdisk cavity, fabricated by Si_3N_4. On the other hand, Ref. [10] investigates the entanglement in a hybrid optomechanical system comprising an optical cavity with a mechanical end-mirror and an intracavity Bose-Einstein condensate (BEC). The cavity gives the action of radiation pressure both to the mirror and the BEC. However, there is no direct interaction between the mirror and the BEC. Due to such indirect second-order interaction, atom-mirror entanglement is produced. Results show that the entanglement appears only at extremely low temperatures ($T \approx 10\ \mu$K). In all the quantum systems mentioned above, optomechanical coupling via radiation pressure or a similar type of coupling leads to the entanglement among different components.

Here we propose a scheme for entangling an optical Fabry-Pérot cavity and a nanomechanical resonator beam (NRB) to a high degree. A high-frequency NRB that operates in the GHz range has been reported [11]. For a NRB operating at the fundamental frequency of GHz and at a temperature of 10–100 mK, some interesting phenomena close to or on the verge of the quantum limit may be observed. Now a doubly clamped NRB is placed between two fixed end mirrors of a laser-driven single-sided Fabry-Pérot cavity. The cavity field does not interact directly with the NRB, but it interacts with a quantum dot in the cavity which couples with the NRB. There are different ways to realize the coupling between a quantum dot and a NRB. For example, a quantum dot (charge qubit) is coupled to the motion of a NRB via electrostatic forces. The NRB also interacts with a toroidal cavity via evanescent coupling. Then an effective qubit-light interface can be realized [12,13]. For another example, we can embed a self-assembled InAs quantum dot in a NRB. Flexion induces extensions and compressions in the NRB. This longitudinal strain will modify the energy of the electronic states confined in the quantum dot through deformation potential coupling [14–16]. The quantum dot can be modeled as a two-level system consisting of the ground state $|g\rangle$ and the single-exciton state $|e\rangle$. By means of this quantum dot, the entanglement between the optical cavity and the NRB can be generated.

The paper is organized as follows. In Sec. II, the model Hamiltonian is introduced and the quantum Langevin equations (QLEs) of the system are derived. We linearize the QLEs and investigate the steady-state optomechanical entanglement by using the logarithmic negativity. Numerical results and discussions are presented in Sec. III. Conclusions are given in Sec. IV.

II. MODEL AND CALCULATIONS

The model considered is illustrated in Fig. 1, where a doubly clamped NRB is placed between two fixed end mirrors of an optical Fabry-Pérot cavity. Because the NRB is geometrically different from a vibrating dielectric membrane or a movable mirror in the cavity [17] and light is reflected back inefficiently, it is not necessary to take the light radiation pressure into consideration. Also, for the vibration frequency chosen in this paper, numerical calculations show that little entanglement can be produced between a dielectric membrane or a movable mirror with the cavity field via the light radiation pressure.

*yxz@sjtu.edu.cn

 ©2013 American Physical Society

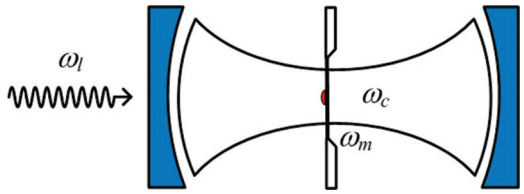

FIG. 1. (Color online) A doubly clamped nanomechanical resonator beam, oscillating at frequency ω_m, interacts via longitudinal strain with an embedded quantum dot which is coupled to a cavity field of frequency ω_c. The cavity is also driven by a laser of frequency ω_l.

Here a quantum dot embedded in the NRB interacts with both the cavity field and the NRB. The total Hamiltonian of the system can be written as

$$H = H_0 + H_{\rm int} + H_{\rm dri}, \tag{1}$$

where H_0 is the free evolution term, $H_{\rm int}$ is the interaction term, and $H_{\rm dri}$ is the laser-driven term. They can be written as [14–16]

$$H_0 = \hbar\omega_c c^+c + \frac{\hbar\omega_m}{2}(p^2+q^2) + \hbar\omega_q S^z, \tag{2}$$

$$H_{\rm int} = \hbar G S^z q + \hbar g(S^+c + S^-c^+), \tag{3}$$

$$H_{\rm dri} = i\hbar\varepsilon(c^+e^{-i\omega_l t} - ce^{i\omega_l t}), \tag{4}$$

where q and p are the NRB displacement and momentum operators while ω_m is its oscillation frequency. c and c^+ are, respectively, the annihilation and creation operators of the cavity mode with frequency ω_c and damping rate κ. $g(G)$ is the coupling strength between the cavity field (NRB) and the quantum dot with exciton frequency ω_q. $\varepsilon = \sqrt{2P\kappa/\hbar\omega_l}$ describes the pumping of the cavity, where P is the power of the input laser with frequency ω_l. The two-level exciton can be characterized by the pseudospin-1/2 operators S^z, S^-, and S^+, which satisfy the commutation relations $[S^+,S^-] = 2S^z$ and $[S^z,S^\pm] = \pm S^\pm$. In a rotating frame at the laser frequency ω_l, the total Hamiltonian is given by

$$\begin{aligned} H =& \hbar(\omega_c-\omega_l)c^+c + \frac{\hbar\omega_m}{2}(p^2+q^2) \\ &+\hbar(\omega_q-\omega_l)S^z + \hbar G S^z q \\ &+\hbar g(S^+c + S^-c^+) + i\hbar\varepsilon(c^+ - c). \end{aligned} \tag{5}$$

Using the Heisenberg equations of motion and including the effects of damping and noises, the resulting QLEs can be written as

$$\dot q = \omega_m p, \tag{6a}$$

$$\dot p = -\omega_m q - GS^z - \gamma_m p + \xi, \tag{6b}$$

$$\dot c = -[\kappa + i(\omega_c-\omega_l)]c - igS^- + \varepsilon + \sqrt{2\kappa}c_{\rm in}, \tag{6c}$$

$$\dot S^z = ig(c^+S^- - cS^+) - \Gamma_1\left(S^z + \tfrac{1}{2}\right), \tag{6d}$$

$$\dot S^- = 2igcS^z - i(\omega_q-\omega_l+Gq)S^- - \Gamma_2 S^-, \tag{6e}$$

where $\xi(t)$ is the quantum Brownian noise acting on the NRB; its correlation function can be written as [18]

$$\langle\xi(t)\xi(t')\rangle = \frac{\gamma_m}{\omega_m}\int\frac{d\omega}{2\pi}e^{-i\omega(t-t')\omega}\left[\coth\left(\frac{\hbar\omega}{2k_BT}\right)+1\right], \tag{7}$$

where k_B is the Boltzmann constant and T is the environment temperature of the NRB. $c_{\rm in}(t)$ is the input vacuum noise operator, which obeys the following correlation functions in the time domain [19]:

$$\langle c_{\rm in}(t)c_{\rm in}^+(t')\rangle = \delta(t-t'), \tag{8}$$

$$\langle c_{\rm in}(t)c_{\rm in}(t')\rangle = \langle c_{\rm in}^+(t)c_{\rm in}^+(t')\rangle = 0. \tag{9}$$

Also γ_m is the mechanical damping rate and Γ_1 (Γ_2) is the exciton relaxation (dephasing) rate. To deal with the QLEs, we assume that the dynamics of the system demonstrates fluctuations around a certain classical steady state. Each operator of the system can be decomposed as the sum of its steady-state value and a small fluctuation, i.e., $q = q_s + \delta q$, $p = p_s + \delta p$, $c = c_s + \delta c$, $S^z = S^z_s + \delta S^z$, and $S^- = S_s + \delta S^-$. By setting all the time derivatives in Eqs. (6) to zero, we finally have the steady-state solution of the system as

$$p_s = 0, \tag{10a}$$

$$q_s = -\frac{GS^z_s}{\omega_m}, \tag{10b}$$

$$S^z_s = -\frac{\Gamma_1\Gamma_2^2 + \Delta_q^2\Gamma_1}{2\Gamma_1\Gamma_2^2 + 2\Delta_q^2\Gamma_1 + 8g^2\Gamma_2|c_s|^2}, \tag{10c}$$

$$c_s = \frac{\varepsilon}{\kappa + i\Delta_c + igw}, \tag{10d}$$

$$S_s = wc_s, \tag{10e}$$

$$w = -ig\Gamma_1\frac{\Gamma_2 - i\Delta_q}{\Gamma_1\Gamma_2^2 + \Delta_q^2\Gamma_1 + 4g^2\Gamma_2|c_s|^2}, \tag{10f}$$

where $\Delta_c = \omega_c - \omega_l$ and $\Delta_q = \omega_q - \omega_l + Gq_s$ are, respectively, the detuning of the optical cavity and the effective detuning of the quantum dot. The QLEs for the fluctuations are

$$\delta\dot q = \omega_m\delta p, \tag{11a}$$

$$\delta\dot p = -\omega_m\delta q - G\delta S^z - \gamma_m\delta p + \xi, \tag{11b}$$

$$\delta\dot c = -i\Delta_c\delta c - ig\delta S^- - \kappa\delta c + \sqrt{2\kappa}c_{\rm in}, \tag{11c}$$

$$\begin{aligned}\delta\dot S^z =& ig(c_s^*\delta S^- - c_s\delta S^+ + S_s\delta c^+ - S_s^*\delta c) \\ &+ ig(\delta c^+\delta S^- - \delta c\delta S^+) - \Gamma_1\delta S^z,\end{aligned} \tag{11d}$$

$$\begin{aligned}\delta\dot S^- =& 2ig\left(c_s\delta S^z + S_s^z\delta c\right) + 2ig\delta c\delta S^z - i\Delta_q\delta S^- \\ &- iG\delta q\delta S^- - iGS_s\delta q - \Gamma_2\delta S^-.\end{aligned} \tag{11e}$$

For the case of $|c_s| \gg 1$, the terms $\delta c^+\delta S^-$ and $\delta c\delta S^+$ in Eq. (11d) and $\delta c\delta S^z$ in Eq. (11e) can be neglected. A similar approximation is used to linearize the corresponding QLEs in Refs. [1–10,20]. The effective detuning of the quantum dot (Δ_q) is fixed at ω_m. The fluctuation δq is sensitive to the temperature and resonator oscillation frequency. Here we chose parameters such that $G\sqrt{\langle\delta q^2\rangle}/\omega_m \ll 1$ (typically, $G/\omega_m < 0.06$). Under those conditions, compared with the term $i\Delta_q\delta S^-$, the term $iG\delta q\delta S^-$ can be neglected in Eq. (11e).

Later numerical calculations also show the reliability of this neglect of the term $iG\delta q\delta S^-$. Then the linearized QLEs for the fluctuations become

$$\delta\dot{q} = \omega_m \delta p, \tag{12a}$$

$$\delta\dot{p} = -\omega_m \delta q - G\delta S^z - \gamma_m \delta p + \xi, \tag{12b}$$

$$\delta\dot{c} = -i\Delta_c \delta c - ig\delta S^- - \kappa\delta c + \sqrt{2k}c_{\rm in}, \tag{12c}$$

$$\delta\dot{S}^z = ig(c_s^*\delta S^- - c_s\delta S^+ + S_s\delta c^+ - S_s^*\delta c) - \Gamma_1\delta S^z, \tag{12d}$$

$$\delta\dot{S}^- = 2ig\left(c_s\delta S^z + S_s^z\delta c\right) - i\Delta_q\delta S^- - iGS_s\delta q - \Gamma_2\delta S^-. \tag{12e}$$

Using the vector of quadrature fluctuations $u^T = (\delta q,\delta p,\delta X,\delta Y,\delta U,\delta V)$, where $\delta X = (\delta c + \delta c^+)/\sqrt{2}$, $\delta Y = (\delta c - \delta c^+)/i\sqrt{2}$, $\delta U = (\delta S^- + \delta S^+)/\sqrt{2}$, and $\delta V = (\delta S^- - \delta S^+)/i\sqrt{2}$, we can rewrite Eqs. (12) compactly as

$$\dot{u}(t) = Au(t) + \eta(t), \tag{13}$$

where the drift matrix A is given by

$$A = \begin{pmatrix} 0 & \omega_m & 0 & 0 & 0 & 0 & 0 \\ -\omega_m & -\gamma_m & 0 & 0 & -G & 0 & 0 \\ 0 & 0 & -\kappa & \Delta_c & 0 & 0 & g \\ 0 & 0 & -\Delta_c & -\kappa & 0 & -g & 0 \\ 0 & 0 & ig\frac{S_s - S_s^*}{\sqrt{2}} & g\frac{S_s + S_s^*}{\sqrt{2}} & -\Gamma_1 & -ig\frac{c_s - c_s^*}{\sqrt{2}} & -g\frac{c_s + c_s^*}{\sqrt{2}} \\ -iG\frac{S_s - S_s^*}{\sqrt{2}} & 0 & 0 & -2gS_s^z & 2ig\frac{c_s - c_s^*}{\sqrt{2}} & -\Gamma_2 & \Delta_q \\ -G\frac{S_s + S_s^*}{\sqrt{2}} & 0 & 2gS_s^z & 0 & 2g\frac{c_s + c_s^*}{\sqrt{2}} & -\Delta_q & \Gamma_2 \end{pmatrix}. \tag{14}$$

The vector of noises η is given by $\eta^T = (0,\xi,\sqrt{2\kappa}\delta X_{\rm in},\sqrt{2k}\delta Y_{\rm in},0,0,0)$, where $\delta X_{\rm in} = (\delta c_{\rm in} + \delta c_{\rm in}^+)/\sqrt{2}$ and $\delta Y_{\rm in} = (\delta c_{\rm in} - \delta c_{\rm in}^+)/i\sqrt{2}$.

The system is stable and reaches a steady state only if all the eigenvalues of the drift matrix A possess negative real parts. The stability conditions can be explicitly derived by applying the Routh-Hurwitz criteria [21]. However it is too complex to give here. Instead we will guarantee the stability of the system via a numerical method, i.e., for all the parameters chosen in this paper, all the eigenvalues of the drift matrix A must possess negative real parts. Since all the noises belong to quantum Gaussian noises and the dynamics of the fluctuations is linearized, the steady state of the system is a zero-mean Gaussian state [2]. Here a 7×7 covariance matrix V is used to extract various correlation information from our system. Its matrix elements are defined as

$$V_{ij} = \frac{\langle u_i(\infty)u_j(\infty) + u_j(\infty)u_i(\infty)\rangle}{2}. \tag{15}$$

For a stable system, we have [1,2]

$$V_{ij} = \sum_{k,l}\int_0^\infty ds \int_0^\infty ds' M_{ik}(s)M_{jl}(s')\Phi_{kl}(s - s'), \tag{16}$$

where $M(s) = \exp(As)$ and $\Phi(s - s')$ is the diffusion matrix, defined as $\Phi_{kl}(s - s') = \langle \eta_k(s)\eta_l(s') + \eta_l(s)\eta_k(s')\rangle/2$. Using the NRB with a large mechanical quality factor ($Q = \omega_m/\gamma_m \gg 1$), we have

$$\Phi(s - s') = D\delta(s - s'), \tag{17}$$

where

$$D = {\rm diag}[0,\gamma_m(2n + 1),\kappa,\kappa,0,0,0] \tag{18}$$

and

$$n = \frac{1}{\exp(\hbar\omega_m/k_BT) - 1} \tag{19}$$

is the thermal mean-occupation number of the mechanical state. Then we can simplify Eq. (16) as [1,2]

$$V = \int_0^\infty ds\, M(s)DM^T(s). \tag{20}$$

When the system is stable, Eq. (20) is equivalent to the following Lyapunov equation:

$$AV + VA^T = -D. \tag{21}$$

To study the entanglement properties of the steady state of the optical cavity and the NRB, we extract a reduced correlation matrix from the covariance matrix V by neglecting the last three rows and columns. This reduced correlation matrix can be expressed as

$$V_{\rm bp} = \begin{pmatrix} B & C \\ C^T & B' \end{pmatrix}, \tag{22}$$

where B, B', and C are 2×2 matrices. We use the logarithmic negativity [22,23] to measure the entanglement between the optical cavity and the NRB, which is given by

$$E_N = \max[0, -\ln(2\eta^-)], \tag{23}$$

where η^- is the symplectic eigenvalue of the matrix $V_{\rm bp}$ and it is given by the equation

$$\eta^- = \frac{1}{\sqrt{2}}\left[\sum(V_{\rm bp}) - \sqrt{\sum(V_{\rm bp})^2 - 4\det V_{\rm bp}}\right], \tag{24}$$

with $\sum(V_{\rm bp}) = \det B + \det B' - 2\det C$.

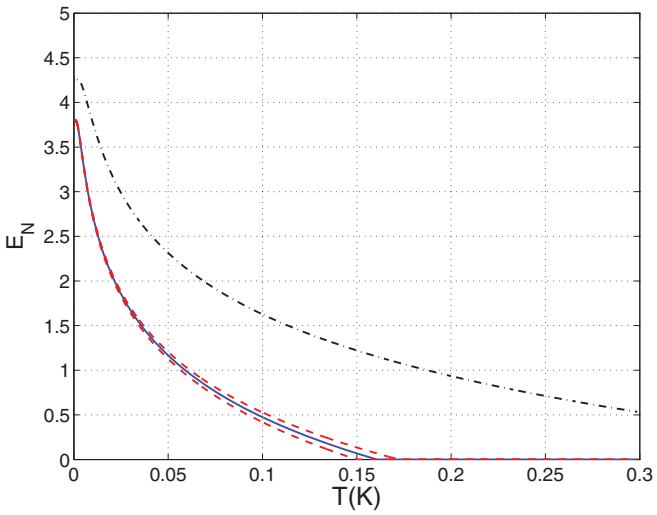

FIG. 2. (Color online) Logarithmic negativity of the optical cavity and the NRB as a function of temperatures for resonator oscillation frequencies $\omega_m/2\pi = 300$ MHz (dot-dashed curve) and $\omega_m/2\pi = 150$ MHz (solid curve; iteration method, dashed curves). Other parameters are $G/\omega_m = 0.06$, $Q = 10^5$, $\kappa = 0.01\omega_m$, $\Delta_c = \Delta_q = \omega_m$, $\Gamma_1 = 0.6$ GHz, $\Gamma_2 = 0.3$ GHz, $P = 30$ mW, and $g = 0.4$ MHz.

III. RESULTS AND DISCUSSION

To illustrate the numerical results, we chose the realistic system of a Fabry-Pérot cavity and an InAs quantum dot coupled to a GaAs NRB. All the parameters used here are accessible in experiment. The logarithmic negativity of the optical cavity and the NRB as a function of temperature is shown in Fig. 2. The detuning of the optical cavity and the effective detuning of the quantum dot are fixed at $\Delta_c = \Delta_q = \omega_m$, which turns out to be the most convenient choice. The exciton relaxation (dephasing) rate is $\Gamma_1 = 0.6$ GHz ($\Gamma_2 = 0.3$ GHz). The quality factor of the NRB is $Q = 10^5$, while the cavity damping rate is $\kappa = 0.01\omega_m$. The coupling strength between the quantum dot and the cavity field (NRB) is taken as $g = 0.4$ MHz ($G/\omega_m = 0.06$). Also the cavity is driven by a laser with wavelength $\lambda = 810$ nm and power $P = 30$ mW. It is reasonable that the logarithmic negativity increases with decreasing temperature. At temperatures near absolute zero, the value of E_N increases to 4.3 for $\omega_m/2\pi = 300$ MHz and 3.8 for $\omega_m/2\pi = 150$ MHz. The entanglement disappears at a critical temperature T_c which increases with increasing frequency ω_m. It is interesting to notice that the entanglement produced via radiation pressure in Ref. [1] is more robust against temperature than that in our model. The entanglement is shown to persist above a temperature of 20 K, which is several orders of magnitude larger than the ground-state temperature of the mechanical oscillator. However, the entanglement we get is an order of magnitude larger than that in Ref. [1] at extremely low temperatures.

The mechanical frequency we chose is almost two orders of magnitude larger than that presented in Refs. [1,10]. This gives the advantage of reaching the ground state at relatively high temperatures. For $\omega_m/2\pi = 300$ MHz and $T = 0.05$ K in Fig. 2, the value of E_N is 2.34. In such a case, we have $\hbar\omega_m = 2.0 \times 10^{-25}$ J and $k_B T = 6.9 \times 10^{-25}$ J. It is obvious that they are in the same order of magnitude. At extremely low temperatures, the elements of the drift matrix A can be used to provide some information about the entanglement of corresponding systems. Though the radiation-pressure coupling strength G_0 is not strong enough ($\sim 10^3$ Hz), what is relevant is the effective optomechanical coupling strength $G = \sqrt{2}G_0|c_s|$, which is an important element in the drift matrix A. When the optical cavity is intensely driven, G can reach up to 10^7 Hz for experimental parameters, so that the generation of significant optomechanical entanglement becomes possible [1,4]. In our proposal, the cavity gets entangled with the NRB through their interactions with the quantum dot. The coupling strength G between the quantum dot and the NRB can reach up to 10^7–10^8 Hz in experiment. Furthermore, the coupling strength g between the quantum dot and the cavity field is dressed as $-g(c_s + c_s^*)/\sqrt{2}$, $-ig(c_s - c_s^*)/\sqrt{2}$, etc., which are some elements of the drift matrix A. This will be propitious to generate significant entanglement. Therefore, the indirect coupling mediated by the quantum dot is useful to enhance the entanglement in our system at extremely low temperatures ($k_B T < \hbar\omega_m$). However, one gets quite different results with the increase of the environment temperature. In our proposal, the quantum dot is embedded in the NRB. The thermal fluctuations of the NRB exert great influence on the dynamics of the quantum dot [see Eq. (12e)]. Then the interaction between the quantum dot and the cavity field makes a great contribution to the decoherence of the cavity field, apart from the cavity input vacuum noise $c_{\rm in}(t)$ [see Eq. (12c)]. Consequently, the entanglement generated in our system is fragile with respect to the temperature.

To show the reliability of neglecting the term $iG\delta q\delta S^-$ in Eq. (11e), we first replace δq in Eq. (11e) by $\pm\sqrt{\langle\delta q^2\rangle} = \pm\sqrt{V_{11}}$, where V_{11} is calculated from the linear QLEs in Eqs. (12). Then Eqs. (11) become a set of new linear QLEs (the terms $\delta c^+\delta S^-$, $\delta c\delta S^+$, and $\delta c\delta S^z$ have been neglected). We get two new values of V_{11} from the new linear QLEs and take a second replacement. We find the results converge quickly, i.e., the so called iteration method is used here. The two dashed curves in Fig. 2 are results of using the iteration method for $\omega_m/2\pi = 150$ MHz. As expected, at low temperature the two dashed curves overlap closely with the solid curve, which is obtained from the linear QLEs in Eqs. (12). With the increase of the temperature, two dashed curves gradually move away from the solid curve. However, results show that our approximation works well for the chosen parameters. For $G/\omega_m = 0.06$ and $T = 0.02$ K, $\sqrt{\langle\delta q^2\rangle} = \sqrt{V_{11}} = 0.18$. If $T = 0.2$ K, $\sqrt{\langle\delta q^2\rangle} = \sqrt{V_{11}} = 0.56$. We see that $G\sqrt{\langle\delta q^2\rangle}/\omega_m \ll 1$. It is therefore reasonable to neglect the term $iG\delta q\delta S^-$ and linearize the QLEs.

Figure 3 illustrates the logarithmic negativity of the optical cavity and the NRB as a function of the coupling strength between the quantum dot and the NRB for different temperatures. If the coupling strength is small enough ($G \leqslant G_c$), there is no entanglement between the optical cavity and the NRB. For $G > G_c$, the entanglement appears and increases with the increase of the coupling strength. The critical point G_c is a special value of the coupling strength, which separates two states of the system, i.e., nonentanglement and entanglement. The entanglement between the cavity and the NRB is generated by their common interaction with the

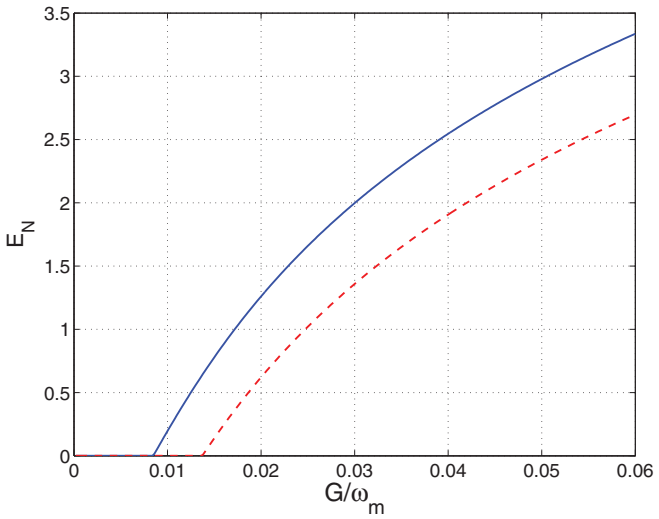

FIG. 3. (Color online) Logarithmic negativity of the optical cavity and the NRB as a function of the coupling strength between the NRB and the quantum dot for temperatures $T = 0.01$ K (solid curve) and $T = 0.02$ K (dashed curve). The resonator oscillation frequency is fixed at $\omega_m/2\pi = 200$ MHz, while the other parameters are those of Fig. 2.

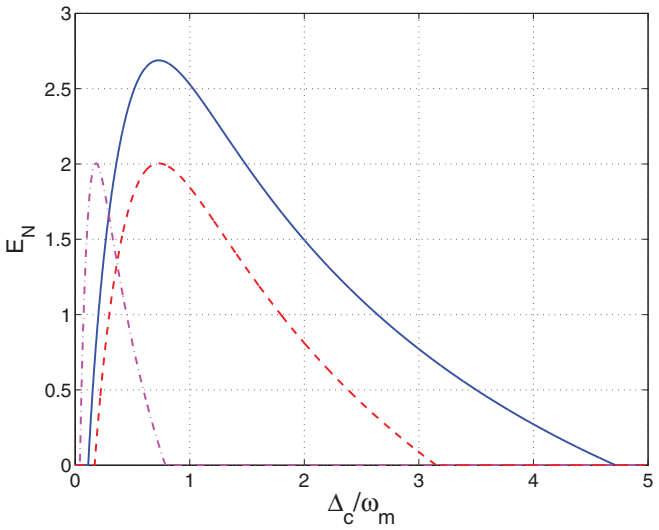

FIG. 4. (Color online) Logarithmic negativity of the optical cavity and the NRB as a function of the detuning of the optical cavity. $\omega_m/2\pi = 400$ MHz, $g = 0.4$ MHz, $T = 0.05$ K (solid curve), and $T = 0.1$ K (dashed curve). The dot-dashed curve corresponds to $T = 0.1$ K and $g = 0.1$ MHz. The other parameters are those of Fig. 2.

quantum dot. Therefore, the strong-coupling strength between the quantum dot and the NRB is favorable for generating high cavity-NRB entanglement. This is not the case for the coupling strength g. Numerical calculations show that there is an optimal coupling strength g which depends on other experimental parameters. From the steady-state solution in Eqs. (10), we get the relation between q_s and $|c_s|^2$ as

$$q_s = \frac{G\left(\Gamma_1\Gamma_2^2 + \Delta_q^2\Gamma_1\right)}{2\omega_m\left(\Gamma_1\Gamma_2^2 + \Delta_q^2\Gamma_1 + 4g^2\Gamma_2|c_s|^2\right)}, \tag{25}$$

which demonstrates indirect correlation between the cavity field and the NRB. It is obvious that the correlation becomes weak as the coupling strength g approaches two extreme (very small or very large) values. Therefore, there exists an optimal coupling strength g as a result of the tradeoff between various parameters. In Fig. 4, we investigate the dependence the entanglement of the optical cavity and the NRB versus the detuning of the optical cavity for different temperatures. As expected, the entanglement decreases at increasing temperatures. A maximal entanglement is reached near $\Delta_c = 0.8\omega_m$. However, this extreme value point depends on many factors, such as the power of the input laser P, the NRB oscillation frequency ω_m, and the coupling strength g. For example, the detuning Δ_c corresponding to the extreme value point decreases with the decrease of the coupling strength g. The entanglement is present only within a finite interval of values of Δ_c, which shrinks with the decrease of the coupling strength g. When g becomes extremely small, the extreme value point moves to a region near $\Delta_c = 0$. One can provide an intuitive explanation of the above behavior. When the coupling strength g decreases from its optimal value (all parameters are fixed except g), the elements of the drift matrix A, which contain g, also decrease. The entanglement between the cavity field and the NRB decreases at the same time. However, if the detuning of the optical cavity Δ_c also decreases, things will be different. According to Eq. (10d), i.e., $c_s = \varepsilon/(\kappa + i\Delta_c + igw)$, where $\kappa \ll \omega_m$, $g \ll \omega_m$, $|w| < 1$, and $\varepsilon \gg \omega_m$ for the parameters chosen, it is obvious that $|c_s|$ becomes extremely large for $\Delta_c \longrightarrow 0$. Though the coupling strength g may be small, the elements of the drift matrix A which play an important role in generating the entanglement, such as $|-g(c_s + c_s^*)/\sqrt{2}|$, $|ig(c_s - c_s^*)/\sqrt{2}|$, etc., may still be large. Then the entanglement still persists in a small interval of values of Δ_c near $\Delta_c = 0$. In such case, as shown in Fig. 5, where we chose the coupling strength $g = 0.01$ MHz, the resonance condition for entanglement is $\Delta_q \approx \omega_m$ (also $\Delta_q \approx -\omega_m$). This

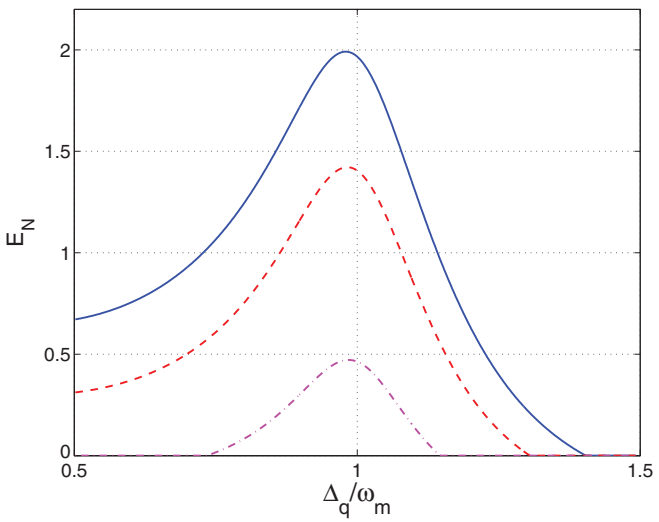

FIG. 5. (Color online) Logarithmic negativity of the optical cavity and the NRB as a function of the effective detuning of the quantum dot. $\omega_m/2\pi = 400$ MHz, $g = 0.01$ MHz, $T = 0.01$ K, $\Delta_c = 1/14\omega_m$ (solid curve), $\Delta_c = 1/10\omega_m$ (dashed curve), and $\Delta_c = 1/5\omega_m$ (dot-dashed curve). The other parameters are those of Fig. 2.

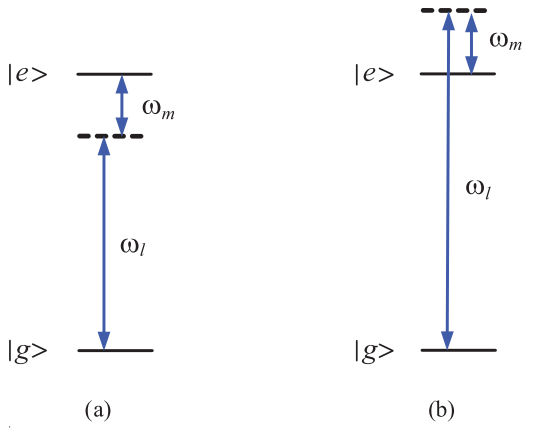

FIG. 6. (Color online) The energy level diagram of the quantum dot with exciton frequency ω_q. The laser frequency ω_l ($\omega_l = \omega_c$) is put into resonance with the red sideband, i.e., $\omega_l = \omega_q - \omega_m$ (a) or the blue sideband, i.e., $\omega_l = \omega_q + \omega_m$ (b) via the coupling between the quantum dot and the NRB.

means that for the case of weak-coupling strength between the cavity and the quantum dot, the entanglement is maximized when the cavity is driven resonantly by a laser of frequency around the red sideband or the blue sideband, i.e., $\omega_c = \omega_l$ and $\omega_l \approx \omega_q \pm \omega_m + Gq_s$ ($Gq_s \ll \omega_m$) (see Fig. 6). This can be explained by solving the dynamics of the pseudospin operators in Eqs. (12) and inserting the solution into Eq. (12c). Then one finds that $ig\delta S^-$ includes an important interaction term of $gGS_s \int_{-\infty}^{t} e^{-\Gamma_2(t-s)} e^{-i\Delta_q(t-s)} \delta q(s) ds$, which demonstrates fluctuation correlation between the cavity field and the NRB (other terms containing g are too complex to give here). It is reasonable to write $\delta q(t)$ as a product of slow variable $\delta q_0(t)$ and fast variable $\sin \omega_m t$, i.e., $\delta q(t) = \delta q_0(t) \sin \omega_m t$. When $\Delta_q \approx \pm\omega_m$, this interaction term is resonantly large. If this condition is not satisfied, the time-dependent kernel $e^{i(\Delta_q \pm \omega_m)t}$ rapidly oscillates and the interaction term tends to average to zero [2]. The resonant condition shown in Fig. 6 makes the indirect coupling of the mechanical oscillation to the cavity mode more effective. As a result, the entanglement between the cavity field and the NRB is maximized on both sides of the resonance. In the model where radiation pressure is used to entangle the cavity and mirror, the entanglement is also enhanced when the cavity is put into resonance with the blue sideband, i.e., the effective cavity detuning $\Delta \approx \omega_m$ [1,4]. This can be explained by the results of Refs. [24,25], where the entanglement between a vibrating mirror and two scattered optical sidebands is investigated.

Finally, we briefly discuss the experimental detection of the generated optomechanical entanglement. To obtain the correlations between the cavity field and the NRB, we should measure quadratures of them. For the optical cavity field, quadratures can be directly measured by homodyning the cavity output using a local oscillator with an appropriate phase [1]. For the mechanical quadratures, Ref. [1] considers a second Fabry-Pérot cavity to measure both the position and the momentum of the mirror. However, the NRB is not coupled to the light field directly in my proposal. Therefore, we use a microwave cavity instead, which is capacitively coupled with the NRB [20]. The presence of the microwave cavity affects the dynamics of the NRB. If it is driven by a much weaker intracavity field, its backaction on the mechanical mode can be neglected.

IV. CONCLUSIONS

In summary, we have investigated in detail the stationary continuous-variable entanglement between an optical cavity and a NRB. Thanks to the mediating action of the quantum dot, a high degree of stationary entanglement is established for experimentally feasible parameters. To deal with our system, we adopt a QLE treatment and focus on the stationary quantum fluctuations. We do not use the low excitation limit approximation to bosonize the spin operators, but keep them in the QLEs, which are then linearized reasonably. Increasing the resonator oscillation frequency or decreasing temperature enhances the entanglement between the optical cavity and the NRB. There is a critical point of the coupling strength between the NRB and the quantum dot. The entanglement appears and increases with the increase of the coupling strength only after the coupling strength exceeds this critical point.

ACKNOWLEDGMENTS

The author acknowledges support from the National Science Foundation of China under Grant No. 10874117. The author also thanks MPIPKS for the conference support (ECOQAS11) and ICTP for the invitation.

[1] D. Vitali, S. Gigan, A. Ferreira, H. R. Böhm, P. Tombesi, A. Guerreiro, V. Vedral, A. Zeilinger, and M. Aspelmeyer, Phys. Rev. Lett. **98**, 030405 (2007).
[2] Sh. Barzanjeh, D. Vitali, P. Tombesi, and G. J. Milburn, Phys. Rev. A **84**, 042342 (2011).
[3] M. J. Hartmann and M. B. Plenio, Phys. Rev. Lett. **101**, 200503 (2008).
[4] C. Genes, D. Vitali, and P. Tombesi, Phys. Rev. A **77**, 050307(R) (2008).
[5] S. Huang and G. S. Agarwal, New J. Phys. **11**, 103044 (2009).
[6] Sh. Barzanjeh, M. H. Naderi, and M. Soltanolkotabi, Phys. Rev. A **84**, 063850 (2011).
[7] L. Zhou, Y. Han, J. Jing, and W. P. Zhang, Phys. Rev. A **83**, 052117 (2011).
[8] H. T. Tan and G. X. Li, Phys. Rev. A **84**, 024301 (2011).
[9] C. L. Zou, X. B. Zou, F. W. Sun, Z. F. Han, and G. C. Guo, Phys. Rev. A **84**, 032317 (2011).
[10] B. Rogers, M. Paternostro, G. M. Palma, and G. De Chiara, Phys. Rev. A **86**, 042323 (2012).
[11] X. M. H. Huang, C. A. Zorman, M. Mehregany, and M. L. Roukes, Nature (London) **421**, 496 (2003).

[12] K. Stannigel, P. Rabl, A. S. Sørensen, P. Zoller, and M. D. Lukin, Phys. Rev. Lett. **105**, 220501 (2010).
[13] K. Stannigel, P. Rabl, A. S. Sørensen, M. D. Lukin, and P. Zoller, Phys. Rev. A **84**, 042341 (2011).
[14] I. Wilson-Rae, P. Zoller, and A. Imamoğlu, Phys. Rev. Lett. **92**, 075507 (2004).
[15] J. J. Li and K. D. Zhu, Phys. Rev. B **83**, 245421 (2011).
[16] J. J. Li, W. He, and K. D. Zhu, Phys. Rev. B **83**, 115445 (2011).
[17] K. Jähne, C. Genes, K. Hammerer, M. Wallquist, E. S. Polzik, and P. Zoller, Phys. Rev. A **79**, 063819 (2009).
[18] V. Giovannetti and D. Vitali, Phys. Rev. A **63**, 023812 (2001).
[19] D. F. Walls and G. J. Milburn, *Quantum Optics* (Springer, Berlin, 1994).
[20] D. Vitali, P. Tombesi, M. J. Woolley, A. C. Doherty, and G. J. Milburn, Phys. Rev. A **76**, 042336 (2007).
[21] E. X. DeJesus and C. Kaufman, Phys. Rev. A **35**, 5288 (1987).
[22] G. Vidal and R. F. Werner, Phys. Rev. A **65**, 032314 (2002).
[23] G. Adesso, A. Serafini, and F. Illuminati, Phys. Rev. A **70**, 022318 (2004).
[24] C. Genes, A. Mari, P. Tombesi, and D. Vitali, Phys. Rev. A **78**, 032316 (2008).
[25] S. Pirandola, S. Mencini, D. Vitali, and P. Tombesi, Phys. Rev. A **68**, 062317 (2003).